

A simple scheme for expanding photonic cluster states for quantum information

P. Kalasuwan¹, G. Mendoza^{1,2}, A. Laing¹, T. Nagata^{3,4}, J. Coggins¹,
M. Callaway¹, S. Takeuchi^{3,4}, A. Stefanov⁵, and J. L. O'Brien^{*,1}

¹*University of Bristol, H.H. Wills Physics Laboratory & Department of Electrical and Electronic Engineering, University of Bristol, Merchant Venturers Building, Woodland Road, Bristol, BS8 1UB, UK.*

²*California Institute of Technology, Pasadena, CA 91125, USA.*

³*Research Institute for Electronic Science, Hokkaido University, Sapporo 060-0812, Japan.*

⁴*The Institute of Scientific and Industrial Research, Osaka University, Mihogaoka 8-1, Ibaraki, Osaka 567-0047, Japan*

⁵*Federal Office of Metrology, METAS, Laboratory Time and Frequency, Switzerland.*

(Dated: March 28, 2022)

We show how an entangled cluster state encoded in the polarization of single photons can be straightforwardly expanded by deterministically entangling additional qubits encoded in the path degree of freedom of the constituent photons. This can be achieved using a polarization–path controlled-phase gate. We experimentally demonstrate a practical and stable realization of this approach by using a Sagnac interferometer to entangle a path qubit and polarization qubit on a single photon. We demonstrate precise control over phase of the path qubit to change the measurement basis and experimentally demonstrate properties of measurement-based quantum computing using a 2 photon, 3 qubit cluster state.

Quantum information science¹ promises both profound insights into the fundamental workings of nature as well as new technologies that harness uniquely quantum mechanical behavior such as superposition and entanglement. Perhaps the most profound aspect of both of these avenues is the prospect of a quantum computer—a device which harnesses massive parallelism to gain exponentially greater computational power for particular tasks. In analogy with a conventional computer, quantum computing was originally formulated in terms of quantum circuits consisting of one- and two-qubit gates operating on a register of qubits which are thereby transformed into the output state of a quantum algorithm¹. In 2001 a remarkable alternative was proposed in which the computation starts with a particular entangled state of many qubits—a cluster state—and the computation proceeds via a sequence of single qubit measurements from left to right that ultimately leave the rightmost column of qubits in the answer state².

Of the various physical systems being considered for quantum information science, photons are particularly attractive for their low noise properties, high speed transmission, and straightforward single qubit operations³; and a scheme for non-deterministic but scalable implementation of two-qubit logic gates ignited the field of all-optical quantum computing⁴. In 2004 it was recognized that cluster states offered tremendous advantages for this optical approach^{5,6}: Because preparation of the cluster state can be probabilistic, non-deterministic logic gates are suitable for making it, removing much of the massive overhead associated with near-deterministic logic gates.

Soon after these theoretical developments there were groundbreaking demonstrations of small-scale algorithms operating on four photon cluster states^{7,8}; cluster states of up to six photons were produced^{9,10}; and the importance of high fidelity was quantified¹¹. It has been recognized that encoding cluster states in multiple de-

grees of freedom of photons may provide advantages to computation¹² and has been demonstrated as a promising route to high count rates and larger cluster states^{13,14}. However, these demonstrations have relied on a sandwich source or double pass crystal to create the cluster state, making their production unwieldy, and scalability an issue. Here, we propose and demonstrate a simple scheme which enables a path encoded qubit to be added to any photon in a polarization encoded cluster state. This is achieved using deterministic controlled-phase (CZ) gate between a photon's polarization and path. We use a Sagnac interferometer architecture that provides a stable and practical realization of this scheme and demonstrate simple measurement-based operations on a 2 photon, 3 qubit cluster state with high fidelity.

A standard way to define a cluster state is via a graph where the nodes represent qubits, initially prepared in the $|+\rangle \equiv (|0\rangle + |1\rangle)/\sqrt{2}$ state, and connecting bonds indicate that an entangling controlled-phase (CZ) gate has been implemented between the pair of qubits that they connect, as in Fig. 1(a) (because these CZ gates commute, the order in which they are performed is not important). Adding a path encoded qubit on a photon in a polarization encoded cluster state therefore requires a CZ gate to be implemented between the polarization of the photon and its path, which must have previously been prepared in the $|+\rangle$ state (Fig. 1(c)).

A polarizing beam splitter (PBS), that transmits horizontal and reflects vertical polarizations of light, implements a controlled-NOT (CNOT) gate on the polarization (control qubit) and path (target qubit) of a single photon passing through it (Fig. 1(c)). A CZ gate can be realized by implementing a Hadamard (\hat{H}) gate ($|0\rangle, |1\rangle \leftrightarrow |0\rangle \pm |1\rangle$) on the target qubit before and after a CNOT gate. For a path qubit a \hat{H} can be implemented with a non-polarizing 1/2 beamsplitter (BS). However, preparation of the $|+\rangle$ state of the path (target) qubit

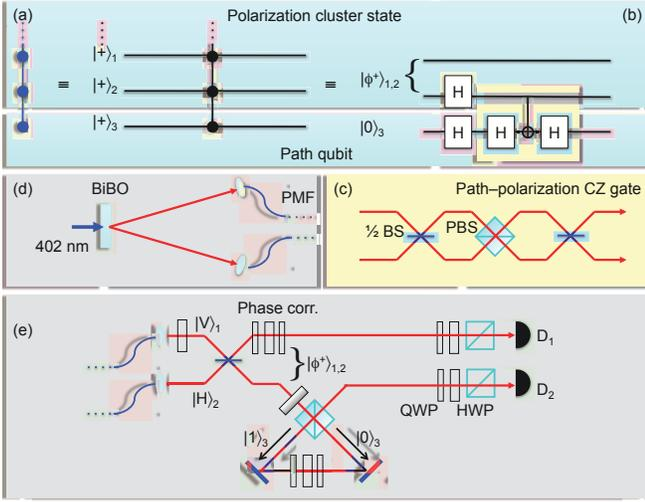


FIG. 1. A simple scheme for adding photon path qubits to a polarization cluster state. (a) The linear three-qubit cluster state can be created by preparing three qubits in the $|+\rangle \equiv |0\rangle + |1\rangle$ state and implementing a two-qubit controlled-phase (CZ) gate between each. (b) The same cluster state can be realized if we start with the state $|\phi^+\rangle_{1,2} |0\rangle_3 \equiv (|00\rangle + |11\rangle)_{1,2} |0\rangle_3$, implement $\hat{H}_2 \otimes \hat{H}_3$, followed by $\text{CZ}_{2,3}$. (c) A controlled-NOT (CNOT) between the path and polarization of a single photon is straightforwardly implemented with a polarizing beam splitter (PBS); a CZ is realized by performing a \hat{H} on the target before and after the CNOT, which for a path qubit is a 1/2 beamsplitter (BS). (d) A pair of photons were produced via Type-I spontaneous parametric downconversion in a non-linear BiBO crystal: a 60 mW 402 nm ‘pump’ laser is shone into the BiBO; a single pump photon can spontaneously ‘split’ into two ‘daughter’ photons, conserving momentum and energy; degenerate pairs of photons are collected into polarization maintaining fibres (PMFs). (e) Implementation of the circuit shown in (c): the polarization entangled state $|\phi^+\rangle_{1,2}$ is realized in post-selection by inputting a horizontal ($|H\rangle$) and vertical ($|V\rangle$) photon into a 1/2 beamsplitter; an \hat{H} on qubit 2, realized with a half waveplate (HWP), converts $|\psi^-\rangle_{1,2}$ to the two qubit cluster state, $(|0+\rangle + |1-\rangle)_{1,2}$; the PBS Sagnac interferometer implements a CZ between the path and polarization of photon 2 (up to a local rotation of the path qubit).

requires an additional \hat{H} , and $\hat{H}\hat{H}$ is the identity operation \hat{I} ; the \hat{H} after the CNOT simply implements a one qubit rotation, and is not included in our demonstration. A PBS is therefore all that is required to add a path qubit to a polarization cluster state. Measuring the path qubit in an arbitrary basis, however, requires a phase shift followed by BS, and so interferometric stability is required.

As a simple demonstration of this approach, we constructed the 3 qubit cluster state

$$|\Phi_3^{lin}\rangle = \frac{1}{\sqrt{2}} (|+\rangle_1 |0\rangle_2 |0\rangle_3 - |-\rangle_1 |1\rangle_2 |1\rangle_3), \quad (1)$$

where the first two qubits were encoded in the polarization of two photons and the third qubit was the path of

the second photon. (Eq. 1 is locally equivalent to the usual 3 qubit linear cluster state; simply with an \hat{H} rotation applied to qubit 3.) Our experimental scheme is shown schematically in Fig. 1(e): Two photons prepared in the state $|1H\rangle_1 |1V\rangle_2$ converge onto a 1/2 beamsplitter, non-deterministically creating the entangled state $|\phi^+\rangle \equiv (|1H\rangle_1 |1H\rangle_2 + |1V\rangle_1 |1V\rangle_2)/\sqrt{2}$, where the number 1 inside the ket brackets indicate photon number and outside subscripts 1 and 2 denote spatial paths. Photon 2 then travels through a half-wave plate set at 22.5° , which implements a \hat{H} on polarization to create the two qubit cluster state. A third qubit is added to the cluster by adding a path degree of freedom on photon 2: Photon 2 enters the Sagnac interferometer via a PBS cube, and forms a superposition of clockwise (C) and counterclockwise (D) paths. The state becomes then

$$|\psi\rangle = (|1H\rangle_1 |1H\rangle_C - |1H\rangle_1 |1V\rangle_D - |1V\rangle_1 |1H\rangle_C - |1V\rangle_1 |1V\rangle_D)/2 \quad (2)$$

The relabeling $|1H\rangle_1 \rightarrow |1\rangle_1$, $|1V\rangle_1 \rightarrow |0\rangle_1$, $|1H\rangle_C \rightarrow |1\rangle_2 |0\rangle_3$, $|1V\rangle_D \rightarrow |0\rangle_2 |1\rangle_3$ gives the state of Eq. 1.

The phase of the path qubit, qubit 3, can be controlled by the quarter and half waveplates (HWPs) inside the Sagnac interferometer; while the stability of this phase is provided by the Sagnac architecture (the visibility of the Sagnac interferometer was 99.5%). The angle α of the HWP in the interferometer sets the relative phase between $|0\rangle_3$ and $|1\rangle_3$ to $e^{i4\alpha}$. The measurement basis of qubit 3 is therefore determined by α .

Following the principles of cluster state quantum computation, an arbitrary qubit rotation can be performed on qubit 3 (path qubit, $j = 3$) by measuring qubits 1 and 2 (polarization qubits) in the basis $B_j(\varphi) \equiv \{|\varphi_+\rangle_j, |\varphi_-\rangle_j\}$ where $|\varphi_\pm\rangle_j \equiv \frac{1}{\sqrt{2}}(|0\rangle_j \pm e^{-i\varphi} |1\rangle_j)$. The eigenvalues $m_j = 0$ or $m_j = 1$ if the measurement outcome on qubit j is $|\varphi_+\rangle_j$ or $|\varphi_-\rangle_j$, respectively. The feed forward information of m_1 selects the projection of the second qubit: for $m_1 = 0$ ($m_1 = 1$) qubit 2 will be projected on $|\varphi_+\rangle_2$ ($|\varphi_-\rangle_2$). After these measurements, qubit 3 is in the state $|\psi\rangle_3 = \sigma_x^{m_2} \sigma_z^{m_1} R_x(\varphi_2) R_z(\varphi_1) |+\rangle$. Hence, the path qubit can be projected into any state (up to a known σ_x operation). The waveplate settings in front of the PBSs determine φ_1 and φ_2 ; simultaneous detection of the two photons at detectors D_1 and D_2 ideally results in a sinusoidal interference fringe, as a function of α , with a phase and amplitude that depends on φ_1 and φ_2 .

Figure 2 shows the density matrix ρ_{exp} , obtained via quantum state tomography, of the polarization state of the two photons after the ordinary BS in Fig. 1(e), before the path qubit is added. (Here the phase correction waveplates were set to produce the singlet state $|\psi^-\rangle \equiv (|01\rangle - |10\rangle)/\sqrt{2}$, rather than $|\phi^+\rangle$). It has a fidelity with the singlet state $|\psi^-\rangle \equiv (|HV\rangle - |VH\rangle)/\sqrt{2}$ of $F = 0.895$. A major source of this non-unit fidelity is that the BS had a reflectivity of $R = 0.59$; the fidelity of ρ_{exp} with the

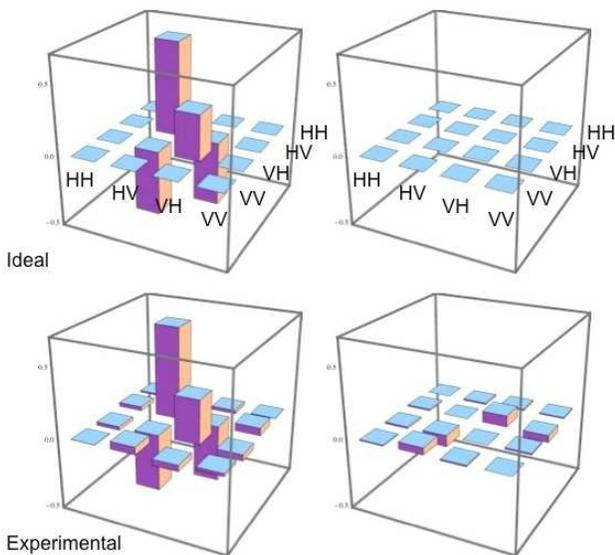


FIG. 2. Real (left) and imaginary (right) parts of the experimentally measured density matrix ρ_{exp} (bottom), which has a fidelity of $F = 0.929$ with expected state $|\psi'\rangle$ (top).

expected output state $|\psi'\rangle \equiv 0.57|HV\rangle + 0.82|VH\rangle$ is $F = 0.929$. The remaining imperfections predominantly arise from the non-unit visibility of quantum interference at the ordinary BS: the measured visibility for two photons of the same polarization was $V_{meas.} = 0.91$, which is $V_{rel.} = 0.97$, relative to the ideal visibility for a $R = 0.59$ BS $V_{ideal} = 0.937$. This visibility results in reduced coherences in the measured density matrix shown in Fig. 2. These imperfections in ρ_{exp} will limit the performance of cluster state operations described below.

Figure 3 shows experimentally measured coincidence counts as a function of α for several different projective measurements on (polarization) qubits 1 and 2: $B_1(\pi/2) \otimes B_2(\pi/2)$ (red), $B_1(\pi/2) \otimes B_2(\pi/4)$ (green), $B_1(\pi/2) \otimes B_2(0)$ (blue) and $B_1(\pi/2) \otimes B_2(-\pi/4)$ (black). The solid lines are theoretical prediction of the fringe expressed as $Y(\alpha) = Y_0(1 + (1 - 2a^2) \cos(4\alpha + \varphi_2) + 2a\sqrt{1 - a^2} \sin(4\alpha + \varphi_2) \sin(\varphi_1))$, where Y_0 is the peak coincidences counts from each experiments and $a (= 0.567)$ is a constant depending on the reflectivity ($R = 0.59$) of the BS. The relation between R and a is $a^2 = (1 - R)^2 / ((1 - R)^2 + R^2)$. The expected high visibility fringes are observed in each case (the non-unit visibility is a result of the reduced coherences in ρ_{exp}), however the phase of each fringe is offset (10's of degrees) compared to the case for a $R = 0.5$ BS but is in good agreement with $Y(\alpha)$. Taking into account the $R = 0.59$ BS well explains these offsets. Similar fringes were measured for other projective measurements on qubits 1 and 2: $\{B_1(-\pi/4), B_1(0), B_1(\pi/4), B_1(\pi/2)\} \otimes \{B_2(-\pi/4), B_2(0), B_2(\pi/4), B_2(\pi/2)\}$ (not shown), and again the observed phases and visibilities were in good agreement with predictions based on an $R = 0.59$ BS. Observation of these fringes confirms the correct one-qubit rotations are realized via the measurements on the two-photon, three-qubit cluster

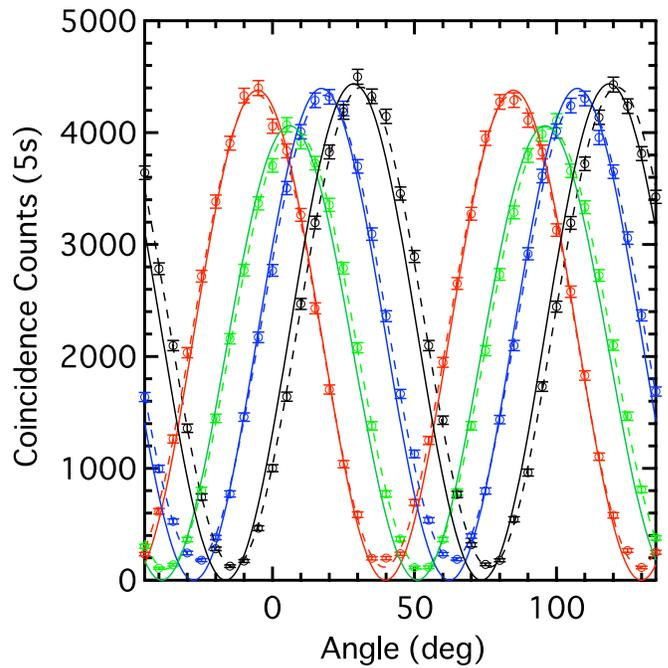


FIG. 3. Path qubit rotation via polarization qubit measurement superimposed on the theoretical curves. The fringes of coincidences counts are pronounced as a function of α as described in the text. The solid lines represent the theoretical prediction given the reflectivity of our BS. The experimental points \circ with errors are fitted by the dashed lines.

state.

We have experimentally demonstrated a simple scheme for adding path-encoded qubits to a polarization-encoded cluster state and demonstrated simple one-qubit rotations on such a hybrid path-polarization cluster state. Similar approaches have used less stable Mach-Zehnder interferometers¹⁵; while 10 qubits on 5 photons have been entangled in a similar way¹⁶. Photonic approaches to exploring cluster states and measurement based quantum computations are currently the most advanced. Further progress is limited by the number of photons, making schemes for encoding more than one qubit per photon appealing. The advent of high performance waveguide integrated quantum circuits^{17,18} that include ultra-stable interferometers^{17,19} and precise optical phase control¹⁹, is a promising architecture for this approach. Our scheme uses entanglement of polarization and path degrees of freedom of one photons. This enables the addition of a path qubit to any photon in a polarization cluster state. The path qubit is not fully connected in the cluster, because the path qubit can be connected to the polarization qubit sharing same photon only. This is most useful at the edges of the cluster state. With current approaches using up to six photons, adding path qubits in this way has the potential to significantly increase the size of cluster states, and thereby the complexity of algorithms that can be implemented. However, there is some possibilities to entangle path qubits from different photons²⁰ to develop more sophisticated cluster state.

We thank T. Rudolph, N. Yoran and X.-Q. Zhou for helpful discussions. This work was supported by IARPA,

EPSRC, QIP IRC and the Leverhulme Trust. G.M. acknowledges support from Caltech's Summer Undergraduate Research Fellowship (SURF).

-
- ¹ M. A. Nielsen and I. L. Chuang *Quantum Computation and Quantum Information* (Cambridge University Press 2000).
- ² R. Raussendorf and H. J. Briegel, *Phys. Rev. Lett.* **86**, 5188 (2001).
- ³ J. L. O'Brien, *Science* **318**, 1567 (2007).
- ⁴ E. Knill, R. Laflamme, and G. J. Milburn, *Nature* **409**, 46 (2001).
- ⁵ M. A. Nielsen, *Phys. Rev. Lett.* **93**, 040503 (2004).
- ⁶ N. Yoran and B. Reznik, *Phys. Rev. Lett.* **91**, 037903 (Jul 2003).
- ⁷ P. Walther, K. J. Resch, T. Rudolph, E. Schenck, H. Weinfurter, V. Vedral, M. Aspelmeyer, and A. Zeilinger, *Nature* **434**, 169 (2005).
- ⁸ R. Prevedel, P. Walther, F. Tiefenbacher, P. Bohi, R. Kaltenbaek, T. Jennewein, and A. Zeilinger, *Nature* **445** 65 (2007).
- ⁹ N. Kiesel, C. Schmid, U. Weber, G. Toth, O. Guhne, R. Ursin, and H. Weinfurter, *Phys. Rev. Lett.* **95**, 210502 (2005).
- ¹⁰ C.-Y. Lu, X.-Q. Zhou, O. Guhne, W.-B. Gao, J. Zhang, Z.-S. Yuan, A. Goebel, T. Yang, and J.-W. Pan, *Nature Physics* **3**, 91 (2007).
- ¹¹ Y. Tokunaga, S. Kuwashiro, T. Yamamoto, M. Koashi, and N. Imoto, *Phys. Rev. Lett.* **100**, 210501 (2008).
- ¹² J. Joo, P. L. Knight, J. L. O'Brien, and T. Rudolph, *Phys. Rev. A* **76**, 052326 (2007).
- ¹³ K. Chen, C.-M. Li, Q. Zhang, Y.-A. Chen, A. Goebel, S. Chen, A. Mair, and J.-W. Pan, *Phys. Rev. Lett.* **99** 120503 (2007).
- ¹⁴ G. Vollone, E. Pomarico, F. D. Martini, and P. Mataloni, *Phys. Rev. Lett.* **100**, 160502 (2008).
- ¹⁵ H. S. Park, J. Cho, J. Y. Lee, D.-H. Lee, and S.-K. Choi, *Opt. Express* **15**, 17960 (2007).
- ¹⁶ W.-B. Gao, C.-Y. Lu, X.-C. Yao, P. Xu., O. Guhne, A. Goebel, Y.-A. Chen, C.-Z. Peng, Z.-B. Chen, and J.-W. Pan(2008).
- ¹⁷ A. Politi, M. J. Cryan, J. G. Rarity, S. Yu, and J. L. O'Brien, *Science* **320**, 646 (2008).
- ¹⁸ G. D. Marshall, A. Politi, J. C. F. Matthews, P. Dekker, M. Ams, M. Withford, and J. L. O'Brien, *Opt. Express* **17**, 12546 (2009).
- ¹⁹ J. C. F. Matthews, A. Politi, A. Stefanov, and J. L. O'Brien, *Nature Photon.* **3**, 346 (2009).
- ²⁰ T. C. Ralph, N. K. Langford, T. B. Bell, and A. G. White, *Phys. Rev. A.* **65**, 062324 (2002).